

Journal of Enzyme Inhibition and Medicinal Chemistry

ISSN: 1475-6366 (Print) 1475-6374 (Online) Journal homepage: https://www.tandfonline.com/loi/ienz20

Synthesis and characterization of a proton transfer salt between 2,6-pyridinedicarboxylic acid and 2-aminobenzothiazole, and its complexes and their inhibition studies on carbonic anhydrase isoenzymes

Halil İlkimen, Cengiz Yenikaya, Musa Sarı, Metin Bülbül, Ekrem Tunca & Hakan Dal

To cite this article: Halil İlkimen, Cengiz Yenikaya, Musa Sarı, Metin Bülbül, Ekrem Tunca & Hakan Dal (2014) Synthesis and characterization of a proton transfer salt between 2,6-pyridinedicarboxylic acid and 2-aminobenzothiazole, and its complexes and their inhibition studies on carbonic anhydrase isoenzymes, Journal of Enzyme Inhibition and Medicinal Chemistry, 29:3, 353-361, DOI: 10.3109/14756366.2013.782299

To link to this article: https://doi.org/10.3109/14756366.2013.782299

View supplementary material

Published online: 01 Jul 2013.

Submit your article to this journal

Article views: 641

View related articles

View Crossmark data

Citing articles: 15 View citing articles

Full Terms & Conditions of access and use can be found at
https://www.tandfonline.com/action/journalInformation?journalCode=ienz20

Journal of Enzyme Inhibition and Medicinal Chemistry

http://informahealthcare.com/enz
ISSN: 1475-6366 (print), 1475-6374 (electronic)

J Enzyme Inhib Med Chem, 2014; 29(3): 353–361
© 2014 Informa UK Ltd. DOI: 10.3109/14756366.2013.782299

informa healthcare

ORIGINAL ARTICLE

Synthesis and characterization of a proton transfer salt between 2,6-pyridinedicarboxylic acid and 2-aminobenzothiazole, and its complexes and their inhibition studies on carbonic anhydrase isoenzymes

Halil İlkimen[1], Cengiz Yenikaya[1], Musa Sarı[2], Metin Bülbül[1], Ekrem Tunca[1], and Hakan Dal[3]

[1]*Department of Chemistry, Faculty of Arts and Sciences, Dumlupınar University, Kütahya, Turkey,* [2]*Department of Physics Education, Gazi University, Ankara, Turkey, and* [3]*Department of Chemistry, Faculty of Science, Anadolu University, Eskişehir, Turkey*

Abstract

A novel proton transfer compound $(HABT)^+(Hdipic)^-$ (**1**) obtained from ABT and H_2dipic and its metal complexes (**2**–**5**) have been prepared and characterized by spectroscopic techniques. Single crystal X-ray diffraction method has also been applied to **2** and **5**. While complex **2** has a distorted octahedral conformation, **5** exhibits a distorted square pyramidal structure. The structures of **3** and **4** might be proposed as octahedral according to experimental data. All compounds were also evaluated for their *in vitro* inhibition effects on hCA I and II for their hydratase and esterase activities. Although there is no inhibition for hydratase activities, all compounds have inhibited the esterase activities of hCA I and II. The comparison of the inhibition studies of **1**–**5** to parent compounds indicates that **1**–**5** have superior inhibitory effects. The inhibition effects of **2**–**5** are also compared to inhibitory properties of the metal complexes of ABT and H_2dipic, revealing an improved transfection profile.

Keywords

2-Aminobenzothiazole, carbonic anydrase, dipicolinic acid, inhibition, proton transfer

History

Received 23 January 2013
Revised 1 March 2013
Accepted 1 March 2013
Published online 26 June 2013

Introduction

Benzothiazole derivatives and their simple metal complexes have been extensively studied and found to have a diverse chemical reactivity and a broad spectrum of biological activities, such as antitumor agents[1–3], antimicrobial[1,4,5], antifungal[1,6,7], analgesics[1,8], anti-inflammatory[1,9], anti-HIV[10,11] and local anesthestics[12]. In recent studies, the mixed ligand metal complexes between 2-aminobenzothiazole and other ligand, such as 7-oxabicyclo[2.2.1]heptane-2,3-dicarboxylic acid[13], picric acid[14], succinic acid[15], formic acid[16], p-chlorophenoxyacetic acid[17], dichloroacetic acid and trifloroacetic acid[18] have been reported in literature. The metal complexes with mixed ligands of these compounds have shown better biological activities than the simple ones[19–22]. Two types of ligands, generally acids and bases, are brought together before coordination with the metal ion in order to prepare the mixed ligand complex compounds[23–26].

Pyridine-2,6-dicarboxylic acid (or dipicolinic acid) (H_2dipic) forms stable chelates with simple metal ions and oxometal cations and can display a widely varying coordination behavior, functioning as a multidentate ligand. Dipicolinates (dipic) commonly coordinate with transition metals by either carboxylate bridges between metal centers, to form polymeric or dimeric complexes, or by tridentate (O, N, O′) chelation to one metal ion[23] in simple or mixed ligand complexation. Dipicolinic acid is also known for its diverse biological activities[27–29].

In this study, a novel proton transfer compound $(HABT)^+(Hdipic)^-$ (**1**) between 2-aminobenzothiazole (ABT) and H_2dipic, namely 2-aminobenzothiazol-3-ium pyridinium-2,6-dicarboxylate and its complexes, $(HABT)[Fe(dipic)_2]\cdot 4H_2O$ (**2**), $(HABT)_2[Co(dipic)_2]\cdot 5H_2O$ (**3**), $(HABT)_2[Ni(dipic)_2]\cdot 4H_2O$ (**4**) and $[Cu(dipic)(ABT)(H_2O)]$ (**5**), have been prepared and characterized by elemental, spectral (^{1}H-NMR, IR and UV-Vis), thermal analyses, magnetic measurements and molar conductivity. Single crystal X-ray analyses of the complexes (**2** and **5**) were also reported.

Furthermore, we have investigated the potential use of these compounds as new inhibitors of human carbonic anhydrase (hCA I and hCA II) isoenzymes in the treatment of glaucoma, which is a group of diseases characterized by the gradual loss of visual field due to an elevation in intraocular pressure (IOP) and which is the second leading cause of blindness worldwide[30,31]. The carbonic anhydrase enzyme (CA; EC.4.2.1.1) including the Zn(II) ion catalyzes the reversible hydration of carbon dioxide to bicarbonate and protons, a very simple but critically important physiological reaction for organisms[32–36]. Carbonic anhydrase inhibitors (CAIs) are mainly sulfonamide compounds, such as the commercial ones acetazolamide (AAZ), dorzolamide (DZA) and brinzolamide (BRZ). These compounds are quite powerful inhibitors, but they have many side effects. Therefore the importance of discovering new CAIs has been received increased interest. Synthetic CAIs, which do not contain sulfonamide groups were reported in the literature[37–40]. For example, we have

Address for correspondence: Cengiz Yenikaya, Department of Chemistry, Dumlupınar University, Kütahya, Turkey. E-mail: yenikaya@dumlupinar.edu.tr

also reported the inhibition effect of a Cu(II) complex with a proton transfer salt between 2-amino-6-methylpyridine and 5-sulfosalicylic acid as the non-sulfonamide compound with a quite good inhibition potential on hCA I and II[24]. These findings prompted us to extend our studies to novel complexes of non-sulfonamide compounds.

Experimental

General methods and materials

All chemicals used were analytical reagents and were commercially purchased from Sigma-Aldrich (Munich, Germany). $FeSO_4 \cdot 7H_2O$, $Co(CH_3COO)_2 \cdot 4H_2O$, $Ni(CH_3COO)_2 \cdot 4H_2O$, $Cu(CH_3COO)_2 \cdot H_2O$, 2-aminobenzothiazole and pyridine-2,6-dicarboxylic acid were used as received. Elemental analyses for C, H, N and S were performed on Elementar Vario III EL (Hanau, Germany) and Fe, Co, Ni and Cu were detected with Perkin Elmer Optima 4300 DV ICP-OES (Perkin Elmer Inc., Wellesley, MA). ^{1}H-NMR spectra were recorded using a Bruker DPX FT NMR (500 MHz) spectrometer (Karlsruhe, Germany) ($SiMe_4$ as internal standard and 85% H_3PO_4 as an external standard). FT-IR spectra were recorded in the 4000–400 cm^{-1} region with Bruker Optics, Vertex 70 FT-IR spectrometer using ATR techniques (Ettlingen, Germany). Thermal analyses were performed on a SII Exstar 6000 TG/DTA 6300 model (Shimadzu Co, Kyoto, Japan) using platinum crucible with 10 mg sample. Measurements were taken in the static air, within 30 °C –900 °C temperature range. The UV-Vis spectra were obtained for aqueous solutions of the compounds (10^{-3} M) with a SHIMADZU UV-2550 spectrometer (Shimadzu Co, Kyoto, Japan) in the range of 200–900 nm. Magnetic susceptibility measurements at room temperature were performed using a Sherwood Scientific Magway MSB MK1 (Sherwood Scientific Ltd, Cambridge, UK) model magnetic balance by the Gouy method using $Hg[Co(SCN)_4]$ as calibrant. Molar conductances of the compound were determined in DMSO (10^{-3} M) at room temperature using a WTW Cond 315i/SET Model conductivity meter (Weilheim, Germany).

Synthesis of $(HABT)^+(Hdipic)^-$ (1) and metal complexes (2–5)

A solution of ABT (0.751 g, 5 mmol) in 25 mL ethanol was added to the solution of H_2dipic (0.836 g, 5 mmol) in 25 mL ethanol. The mixture was refluxed for 3 h, and then was cooled to room temperature. The reaction mixture was kept at room temperature for 3 h to give white solid of **1** (1.428 g, 90% yield).

A solution of 1 mmol metal (II) salt [0.139 g $FeSO_4 \cdot 7H_2O$ or 0.1245 g $Co(CH_3COO)_2 \cdot 4H_2O$ or 0.124 g $Ni(CH_3COO)_2 \cdot 4H_2O$ or 0.099 g $Cu(CH_3COO)_2 \cdot H_2O$] in water (10 mL) was added dropwise to the solution of **1** (0.311 g, 1 mmol) in water/ethanol (1:1) (20 mL) with stirring at room temperature for 2 h. The reaction mixture was kept at room temperature for 2 weeks to give orange crystalline solid of complex **2** (0.4570 g, 75% yield) and green crystalline solid of complex **5** (0.5812 g, 60% yield). Other metal complexes were obtained as brown amorphous solid for **3** (0.5081 g, 65% yield) and as green amorphous solid for **4** (0.5725 g, 75% yield) (Figure 1). The prismatic single crystals of **2** and **5** suitable for single X-ray diffraction studies were obtained by recrystallization of **2** and **5** from ethanol/water (1:1) solutions.

Anal. Calcd for **1** ($C_{14}H_{11}N_3O_4S$): C, 52.99%; H, 3.49%; N, 13.24%; S, 10.10%. Found: C, 52.95%; H, 3.51%; N, 13.20%; S, 10.12%; for **2** ($C_{21}H_{23}N_4O_{13}SFe$): C, 40.21%; H, 3.70%; N, 8.93%; S, 5.11%; Fe, 8.90%. Found: C, 40.25%; H, 3.75%; N, 8.90%; S, 5.15%; Fe, 8.70%; for **3** ($C_{28}H_{30}N_6O_{13}S_2Co$): C, 43.03%; H, 3.87%; N, 10.75%; S, 8.20%; Co, 7.54%. Found: C, 43.05%; H, 3.90%; N, 10.73%; S, 8.25%; Co, 7.60%; for **4** ($C_{28}H_{28}N_6O_{12}S_2Ni$): C, 44.05%; H, 3.70%; N, 11.01%; S, 8.40%; Ni, 7.69%. Found: C, 44.00%; H, 3.75%; N, 11.05%; S, 8.37%; Ni, 7.85%; and for **5** ($C_{14}H_{11}N_3O_5SCu$): C, 42.37%; H, 2.79%; N, 10.59%; S, 8.08%; Cu, 16.01%. Found: C, 42.35%; H, 2.75%; N, 10.60%; S, 8.05%; Cu, 16.00%.

In addition, simple metal complexes of ABT (FeABT, CoABT, NiABT and CuABT) and of H_2dipic (Fedipic, Codipic, Nidipic and Cudipic) were synthesized according to the literature in order to compare the inhibition studies with the complex compounds of proton transfer salt[41–43].

*Crystal structure determination of **2** and **5***

The crystal and instrumental parameters used in the unit-cell determination and data collection are summarized in Table 1 for the compounds **2** and **5**. Crystallographic data of **2** and **5** were recorded on a Bruker Kappa APEX II CCD area-detector X-ray diffractometer using graphite monochromatized with MoK_α radiation ($\lambda = 0.71073$ Å), using ω–2θ scan mode. The empirical absorption corrections were applied by multi-scan via Bruker, SADABS software[44]. The structures were solved by the direct method and refined by full-matrix least-squares techniques on F^2 using the solution program SHELXS-97 and refined using SHELXL-97[45]. All non-hydrogen atoms were refined with anisotropic displacement parameters. Hydrogen atoms bonded to the carbon and nitrogen atoms were placed in their calculated idealized positions and refined as riding with C–H = 0.95 Å and N–H = 0.88 Å with $U_{iso}(H) = 1.2U_{eq}(C,N)$. The hydrogen atoms of water molecules were located from difference Fourier maps and refined with O–H distance restraint 0.82(2) Å. The drawings of molecules were accomplished with the help of ORTEP-3 for Windows[46].

Purification of isoenzymes hCA I and II from human erythrocytes

In order to purify hCA I and II isoenzymes, first, human blood was centrifuged at 1500 rpm for 20 min, and after the removal of the plasma, the erythrocytes were washed with an isotonic solution (0.9% NaCl). After that, the erythrocytes were lysed with 1.5 volume of ice-cold water. The lysate was centrifuged at 20 000 rpm for 30 min to remove cell membranes and non-lysed cells. The pH of the supernatant was adjusted to 8.7 with tris and was then loaded onto an affinity column containing Sepharose-4B-L-tyrosine-p-aminobenzene sulfonamide as the binding group. After extensive washing with 25 mM tris–HCl/22 mM Na_2SO_4 (pH 8.7), the hCA I and II isoenzymes were eluted with 1.0 M NaCl/25 mM Na_2HPO_4 (pH 6.3) and 0.1 M CH_3COONa/0.5 M $NaClO_4$ (pH 5.6)[47,48]. The amount of purified protein was estimated by the Bradford method[49] and SDS–PAGE was carried out to determine whether the elute contained the enzyme[50].

Hydratase and esterase activity assay

On hydration of CO_2[51], CO_2-hydratase activity as an enzyme unit (EU) was calculated by using the equation $((t_0 - t_c)/t_c)$, where t_0 and t_c are the times for pH change of the non-enzymatic and the enzymatic reactions, respectively. IC_{50} values (the concentration of inhibitor producing a 50% inhibition of CA activity) have been obtained as *in vitro* for free ligands, ABT and H_2dipic, the simple metal complexes of ABT and H_2dipic, the synthesized compounds **1–5**, and acetazolamide (AAZ) as the control compound for their hydratase and esterase activities.

Carbonic anhydrase esterase activity was assayed by following the change in absorbance at 348 nm of 4-nitrophenylacetate (NPA) to 4-nitrophenylate ion over a period of 3 min at 25 °C using a spectrophotometer (SHIMADZU UV–VIS) according to the method described in the literature[52,53]. The enzymatic

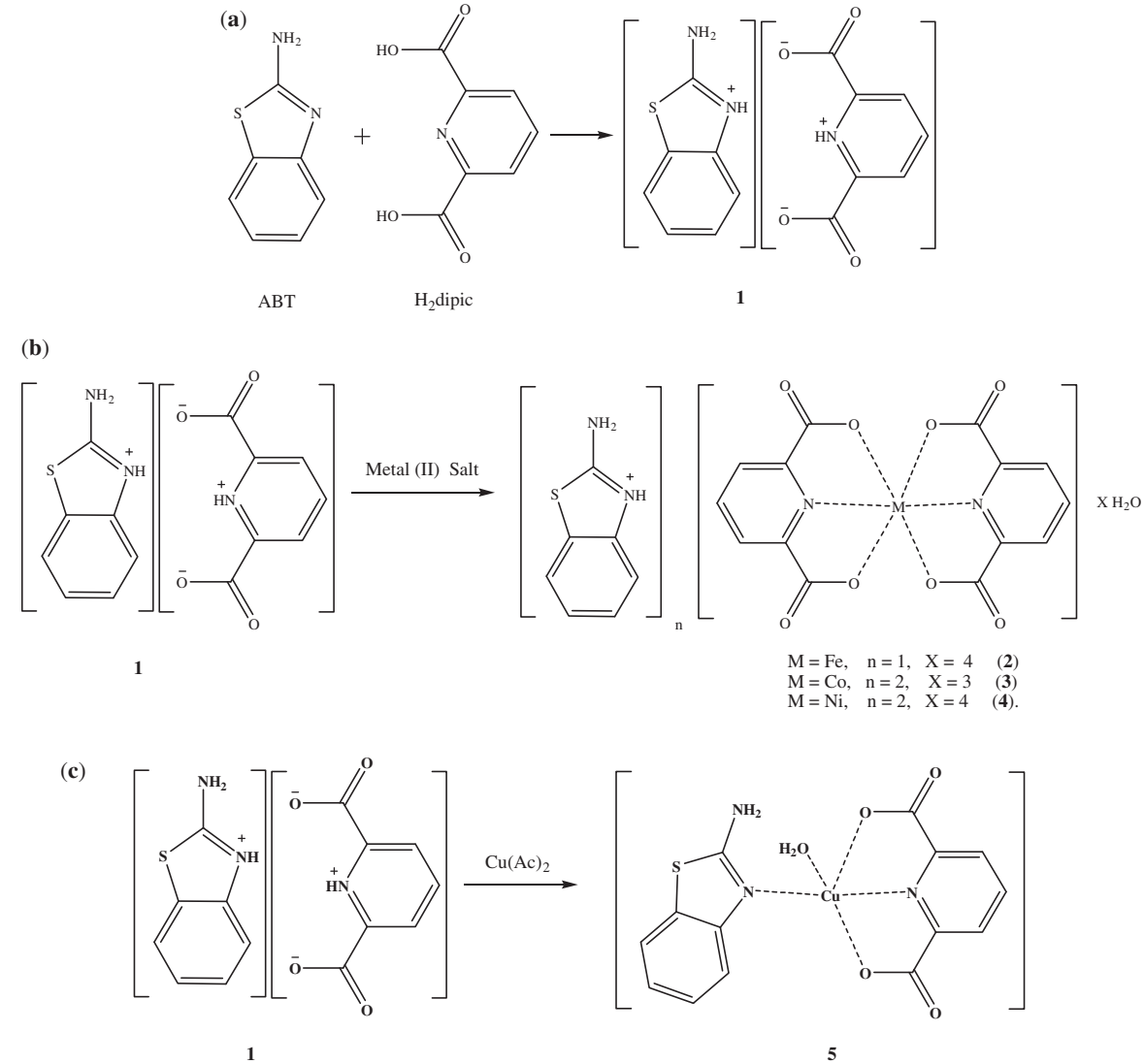


Figure 1. Syntheses of compounds **1**–**5**: (a) for **1**, (b) for **2**–**4** and (c) for **5**.

reaction, in a total volume of 3.0 mL, contained 1.4 mL of 0.05 M tris–SO_4 buffer (pH 7.4), 1 mL of 3 mM 4-nitrophenylacetate, 0.5 mL H_2O and 0.1 mL enzyme solution. A reference measurement was obtained by preparing the same cuvette without enzyme solution.

Results and discussion

Crystal structures of 2 ($C_{21}H_{33}N_4O_{13}SFe$) and 5 ($C_{14}H_{11}N_3O_5SCu$)

The molecular structures of **2** and **5**, with the atom labeling of symmetric units, are shown in Figures 2 and 3, respectively. The details of the crystal structure solutions are summarized in Table 1 and the selected bond lengths and angles are listed in Table 2.

The complex **2**, $(HABT)[Fe(dipic)_2]\cdot 4H_2O$, crystallizes in the monoclinic *C2/c* space group. The structure of **2** consists of one $HABT^+$ cation, one $[Fe(dipic)_2]^-$ anion and four uncoordinated water molecules. In complex **2**, the Fe(III) ion coordinates with four oxygen atoms (O1, O4, O5 and O8) and two nitrogen atoms (N1 and N2) of two pyridine-2,6-dicarboxylate molecules resulting in a distorted octahedral conformation. Both carboxylate oxygen atoms from dipic occupy the *trans*-apical positions of the Fe(III) coordination polyhedron with bond lengths [Fe1–O1 = 1.9961(15) Å, Fe1–O4 = 2.0746(15) Å, Fe1–O5 = 1.9994(18) Å and Fe1–O8 = 2.0180(16) Å], and define low *trans*-angle value around Fe(III) ion as 151.13(7)° for O1–Fe1–O4, which reveals a rather rigid structure of such tri-dentate ligands. In contrast, the N1–Fe1–N2 *trans*-angle is much closer to 180° (162.68(7)°) and the dihedral angle defined by the mean planes of two dipic ligands is 86.48(12)° showing that they fall almost perpendicular. The Fe1 atom lies at the center of the mean planes. The Fe–N and Fe–O bond distances lie within the expected range of 2.0470(16)–2.0562(17) Å and 1.9961(15)–2.0746(15) Å, respectively (Table 2). In all essential details, the geometry of the molecule regarding bond lengths and angles of the compound are in good agreement with the values observed in similar Fe(III) complexes[54,55].

The complex **5**, [Cu(dipic)(ABT)(H_2O)], crystallizes in the monoclinic *C2/c* space group. The asymmetric unit contains one dipic ion, one ABT molecule, one Cu(II) ion and one coordinated water molecule. The structural index, $\tau = (\beta - \alpha/60)$, was evaluated by the two large angles in the pentacoordinate arrangement, where τ is 0.0 for a regular square pyramidal and 1.0 for a trigonal bipyramidal arrangement ($\alpha < \beta$)[56]. In complex **5**, the coordination arrangement of the Cu(II) ion is slightly distorted from regular square pyramidal since the value of the structural index τ is 0.065. The penta-coordinated central Cu(II) ion resides on a center of symmetry comprising two N atoms, one from dipic (N1) and one from the ABT ring (N2), two carboxylate O atoms from dipic (O1 and O4) and one O atom

Table 1. Crystal data and structure refinement details for compounds **2** and **5**.

	2	**5**
Chemical formula	$C_{21}H_{21}N_4O_{12}SFe$	$C_{14}H_{11}N_3O_5SCu$
Formula weight	609.34	396.88
Temperature (K)	100(2)	115(2)
Wavelength (Å)	0.71073	0.71073
Crystal system, space group	Monoclinic, *C2/c*	Monoclinic, *C2/c*
Unit cell dimensions (Å, °)		
a	18.9865(4)	25.8098(8)
b	10.4654(3)	7.2465(2)
c	25.7499(6)	18.5025(6)
β	97.287(2)	119.6660(10)
Volume (Å^3)	5075.2(2)	3006.95(16)
Z	8	8
Absorption coefficient (mm^1)	0.748	1.753
Calculated density (Mg m^{-3})	1.595	1.623
F(000)	2504	1608
Crystal size (mm)	0.36 × 0.30 × 0.20	0.38 × 0.22 × 0.07
Theta range for data collection (°)	1.59–28.31	1.82–28.42
Limiting indices	$-25 \le h \le 24,\ -13 \le k \le 13,\ -34 \le l \le 33$	$-32 \le h \le 34,\ -9 \le k \le 9,\ -24 \le l \le 15$
Reflections collected	23 695	13 544
Independent reflections	6328	3789
Number of reflections used	4621	3085
Number of parameters	384	242
Max. and min. transmission	0.764, 0.861	0.658, 0.893
Refinement method	Full-matrix least-squares on F^2	Full-matrix least-squares on F^2
Final *R* indices [$I \ge 2\sigma(I)$]	$R_1 = 0.0394$, $wR_2 = 0.0999$	$R_1 = 0.0345$, $wR_2 = 0.0895$
R indices (all data)	$R_1 = 0.0641$, $wR_2 = 0.01175$	$R_1 = 0.0478$, $wR_2 = 0.1122$
Goodness-of-fit on F^2	1.070	1.174
Largest difference in peak and hole (e Å^{-3})	−0.370 and 0.319	−0.561 and 0.787

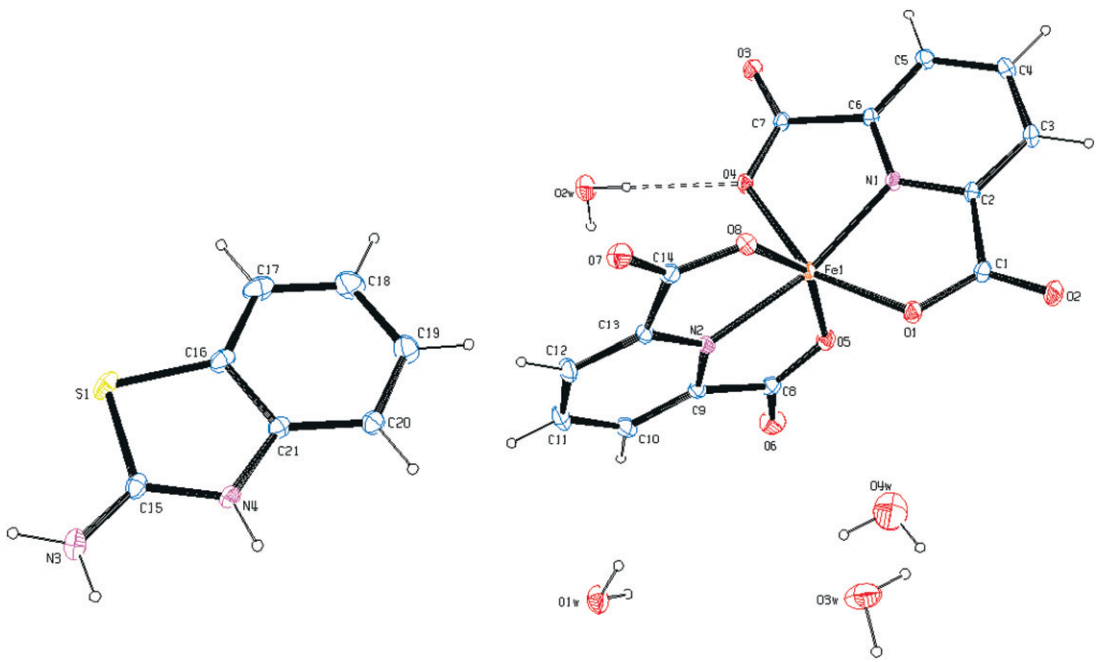


Figure 2. An ORTEP drawing of asymmetric unit of **2** with the atom-numbering scheme. Displacement ellipsoids are drawn at the 40% probability level.

from water (O1w). Two N atoms from two different ligands, dipic and ABT, occupy equatorial positions with Cu–N distances of 1.917(2) and 1.981(2) Å for Cu–N1 and Cu–N2, respectively, and the bond distances are similar to those found in other related Cu(II) complexes[57–59]. The Cu–O bond distances [Cu1–O1 = 2.033(2) and Cu1–O4 = 2.047(2) Å], observed from the carboxylate coordination to the center metal ion, are well consistent with those observed in the literature data[57–59]. The coordination arrangement is characterized by an N1–Cu1–N2 equatorial angle which is 162.79(10) Å. The dihedral angle between the planes of the DPC and ABT is 7.21(10) Å. The Cu1 atom lies −0.1016(14) Å out of the planes. The Cu–O1w bond distance, arising from coordination of the water molecule with the central metal ion, is 2.257(2) Å, which is much longer than the Cu–O (carboxylate) bond distances.

Hydrogen bonds between the carboxylate group and water molecules play important roles in stabilizing the crystal structures. The ranges of the D–H · · · A angles and those of the H · · · A

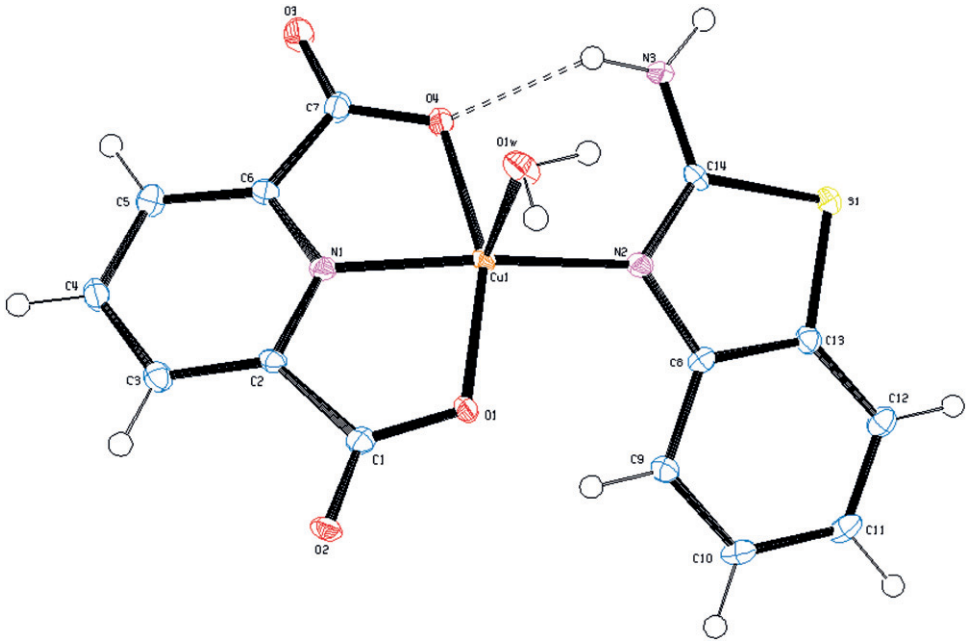


Figure 3. An ORTEP drawing of asymmetric unit of **5** with the atom-numbering scheme. Displacement ellipsoids are drawn at the 40% probability level.

Table 2. Selected bond distances (Å) and angles (°) for compounds **2** and **5**.

Compound **2**					
Fe1–O1	1.9961(15)	Fe1–O5	1.9994(18)	Fe1–N1	2.0562(17)
Fe1–O4	2.0746(15)	Fe1–O8	2.0180(16)	Fe1–N2	2.0470(16)
O1–Fe1–O4	151.13(6)	O4–Fe1–O5	94.02(6)	O5–Fe1–N1	99.14(7)
O1–Fe1–O5	94.62(7)	O4–Fe1–O8	91.25(6)	O5–Fe1–N2	76.24(7)
O1–Fe1–O8	94.10(7)	O5–Fe1–O8	151.59(7)	O8–Fe1–N1	109.18(7)
O1–Fe1–N1	76.68(7)	O4–Fe1–N1	74.77(6)	O8–Fe1–N2	75.98(7)
O1–Fe1–N2	120.03(7)	O4–Fe1–N2	88.79(6)	N1–Fe1–N2	162.68(7)
Compound **5**					
Cu1–N1	1.917(2)	Cu1–O1	2.033(2)	Cu1–O1W	2.257(2)
Cu1–N2	1.981(2)	Cu1–O4	2.047(2)		
N1–Cu1–N2	162.79(10)	N2–Cu1–O4	96.19(9)	O1–Cu1–O1W	87.93(8)
N1–Cu1–O1	79.87(9)	O1–Cu1–O4	158.91(8)	O4–Cu1–O1W	97.05(8)
N2–Cu1–O1	103.58(9)	N1–Cu1–O1W	100.23(9)		
N1–Cu1–O4	79.09(9)	N2–Cu1–O1W	96.76(9)		

Table 3. Hydrogen bonding geometry of compounds **2** and **5** (Å, °).

D–H···A	d(D–H)	d(H···A)	d(D···A)	∠D–H···A
Compound **2**				
O2W–H2A–O4	0.808(17)	2.07(2)	2.858(2)	166(4)
Compound **5**				
N3–H3A–O4	0.88	2.03	2.742(3)	137.7

and D···A distances indicate the presence of strong and weak hydrogen bondings in the structures **2** and **5** (Table 3).

^{1}H NMR studies of $(HABT)^+(Hdipic)^-$ (1)

The ^{1}H-NMR spectra of the compound (**1**) was obtained in d_6-DMSO at room temperature using TMS as internal standard (Figure S1). Table 4 lists complete ^{1}H-NMR assignments for the compound **1**. The ^{1}H signals were assigned on the basis of chemical shifts, multiplicities, intensity of the signals and coupling constants.

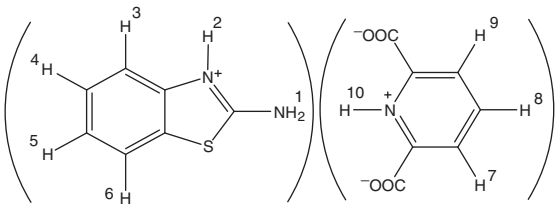
H^5 and H^4 protons of the $(HABT)^+$ ring are triplets with 1H intensity and they are observed at 7.01 (H^5, $^3J_{H5\text{-}H4,6} = 7.51$ Hz) and 7.21 ppm (H^4, $^3J_{H4\text{-}H3,5} = 7.61$ Hz). In addition, H^6 and H^3 protons of the $(HABT)^+$ ring are doublets as expected and found at 7.33 (H^6, $^3J_{H6\text{-}H5} = 7.95$ Hz) and 7.64 ppm (H^3, $^3J_{H3\text{-}H4} = 7.75$ Hz) with 1H intensity. H^8 proton of the $(Hdipic)^-$ ring is a triplet with 1H intensity and observed at 7.91 ppm ($^3J_{H8\text{-}H7,9} = 7.67$ Hz). H^7 and H^9 protons are symmetric and they are observed at 8.25 ppm as doublets with 2H intensity ($^3J_{H7,9\text{-}H8} = 7.71$ Hz). The hydrogen atoms on $-NH_2$ (H^1) and $=N^+$-H_{ABT} (H^2) and $=N^+$-H_{dipic} (H^{10}) in compound **1** were not observed in the ^{1}H NMR spectrum.

The room temperature ^{1}H-NMR spectrum for compound **1** indicates clearly the formation of the proton transfer compound with 1:1 ratio of ABT and H_2dipic (Figure S1).

FT–IR measurements

The infrared spectral data of the starting compounds (ABT and H_2dipic) and compounds **1**–**5** are given in Table S1. In the high frequency region, weak bands 3090–3054 cm^{-1} are attributed to

Table 4. ^{1}H-NMR chemical shifts (ppm) with coupling constants and assignments for compound **1**.



H^5	7.01 (1H, t) [$^3J_{H5\text{-}H4,6} = 7.51$ Hz]
H^4	7.21 (1H, t) [$^3J_{H4\text{-}H3,5} = 7.61$ Hz]
H^6	7.33 (1H, d) [$^3J_{H6\text{-}H5} = 7.95$ Hz]
H^3	7.64 (1H, d) [$^3J_{H3\text{-}H4} = 7.75$ Hz]
H^8	7.91 (1H, t) [$^3J_{H8\text{-}H7,9} = 7.67$ Hz]
H^7, H^9	8.25 (2H, d) [$^3J_{H7,9\text{-}H8} = 7.71$ Hz]
H^1, H^2, H^{10}	Not observed

Table 5. IC_{50} values of esterase activities on hCA I and hCA II isoenzymes.

	Esterase IC_{50} (mM)	
Inhibitor	hCA I	hCA II
AAZ	6.1×10^{-3}	4.5×10^{-3}
H_2dipic	No inhibition	No inhibition
Fedipic	No inhibition	No inhibition
Codipic	No inhibition	No inhibition
Nidipic	No inhibition	No inhibition
Cudipic	No inhibition	No inhibition
ABT	No inhibition	No inhibition
FeABT	0.284	0.257
CoABT	0.313	0.289
NiABT	0.337	0.287
CuABT	0.345	0.301
1	0.746	0.674
2	0.241	0.221
3	0.244	0.236
4	0.276	0.254
5	0.299	0.281

the stretching vibrations of aromatic C–H. There is a broad absorption band at 2900 cm^{-1} attributed to the ν(OH) vibrations of carboxylate group of H_2dipic. This band is not observed in compound **1** due to proton transfer. There are also broad absorption bands at 3465–3390 cm^{-1} attributed to the ν(OH) vibrations of coordinated and uncoordinated water molecules in compounds **2**–**5**. The relatively weak and broad bands at 2771–2508 cm^{-1} are attributed to the $\nu(N^+–H)$ vibration[60] for **1** from $(HABT)^+$ and $(Hdipic)^-$ and for **2**–**4** from $(HABT)^+$. These bands were not observed for compound **5** due to deprotonation of the salt during the complex formation (Figure 2). The absorption bands at 3395 and 3268 cm^{-1} of NH_2 group of ABT are slightly shifted from those found for compound **1** (3382 and 3250 cm^{-1}), for compound **2** (3440 and 3293 cm^{-1}), for compound **3** (3331 and 3218 cm^{-1}), for compound **4** (3390 and 3193 cm^{-1}) and for compound **5** (3371 and 3283 cm^{-1}) due to the weak intermolecular interactions. The carboxylate groups exhibit strong carbonyl bands in the region 1700–1570 cm^{-1}. These bands are reflected by IR spectrum of the asymmetric (ν_{as}) and symmetric (ν_s) stretching vibrations at 1701 and 1456 cm^{-1} for H_2dipic, 1644 and 1468 cm^{-1} for **1**, 1665 and 1469 cm^{-1} for **2**, 1609 and 1466 cm^{-1} for **3**, 1604 and 1467 cm^{-1} for **4** and 1668 and 1453 cm^{-1} for **5**. The differences ($\Delta\nu$) between the asymmetric and symmetric stretches of the carboxylate groups of **2**–**5** are 176, 143, 137 and 215, respectively, which suggest a monodentate binding of the carboxylate group to the metal ion for all complexes[61]. The C–O vibrations data for all compounds are between 1372 and 1080 cm^{-1} as indicated by Ucar et al.[62]. The strong absorption bands at the region of 1640–1415 cm^{-1} are attributed to the ν(C=N) and ν(C=C) vibrations for all compounds. The ring wagging vibrations of the pyridine groups are also observed at 795–679 cm^{-1} region for compounds H_2dipic and **1**–**5**. The weak bands at 638–532 cm^{-1} and 591–429 cm^{-1} are from the M–N and M–O vibrations of compounds **2**–**5**.

Thermal analyses of 1–5

Figures S2–S6 show the TG-DTG and DTA curves of compounds **1**–**5**, respectively, and thermal analyses results are given in Table S2.

For compound **1**, two stages are observed and the first endothermic stage corresponds to the loss of the $C_7H_8N_2SO$ unit. The second exothermic one is the decomposition of the residue of $C_7H_3NO_3$ unit.

For compounds **2**, **3** and **4**, four stages are observed, and the first endothermic stage corresponds to the loss of the four, five and four moles of water, respectively. The second endothermic stage is consistent to the loss of one, two and two moles $(HABT)^+$, respectively. Two moles of $(dipic)^{2-}$ are decomposed exothermically in the third stage for **2**–**4**. The final decomposition products are FeO, CoO and NiO, respectively, and they are identified by IR spectroscopy.

For compound **5**, the first endothermic peak corresponds to the loss of one mole of water. The endothermic second stage is consistent to the loss of the CNH_2 unit. The third stage, an endothermic peak, agrees to the loss of the $C_{11}H_8S$ unit and the $C_2N_2O_3$ unit is decomposed exothermically in the following stage. The final decomposition product is CuO identified by IR spectroscopy.

UV/Vis Spectrum, magnetic susceptibility and molar conductivity

The electronic spectra of compounds **1**–**5**, and the free ligands ABT and H_2dipic were recorded in water/ethanol (1:1) and in DMSO solution (1×10^{-3} M) at room temperature (Table S3). Characteristic π–π* transitions in the range of 224–347 nm for **1**–**5** are observed in water/ethanol and 267–295 nm for **1**–**5** are observed in DMSO. The same π–π* transition profiles are also detected for the free ligands ABT (239, 295 nm in water/ethanol and 243, 289 nm in DMSO) and H_2dipic (299 nm in water/ethanol and 303 nm in DMSO). π–π* transitions of the free ligands do not show any marked differences from those of either proton transfer compound or metal complexes in both solutions. The intensities of the absorption bands for all compounds in DMSO are, in general, higher than in water/ethanol.

The bands for the $d \rightarrow d$ transitions are observed at 803 and 796 nm for **3**, 738 and 776 nm for **4**, which fit for octahedral structure for both[63,64], 779 and 785 nm for **5** in water/ethanol and in DMSO, respectively. The $d \rightarrow d$ transition for complex **2** containing Fe(III) ion with d^5 has not been observed.

The room temperature magnetic moments of the metal complexes are 5.98 for **2**, 3.80 for **3**, 2.81 for **4** and 1.70 BM for **5** per metal ion, indicating the presence of five (d^5), three (d^7), two (d^8) and one (d^9) single electrons, respectively. These results for **3** and **4** agree with the octahedral structures for **3** and **4**.

The molar conductivity data in water/ethanol and in DMSO are 83.4 and 65.3 Ω^{-1}cm^2 mol^{-1} for **2**, 82.2 and 62.1 Ω^{-1}cm^2 mol^{-1} for **3**, 68.7 and 63.6 Ω^{-1}cm^2 mol^{-1} for **4** and 0.8 and 0.9 Ω^{-1}cm^2 mol^{-1} for **5**, respectively, indicating that the complexes **3** and **4** are ionic with a 2:1 ratio, the complex **2** is ionic with a 1:1 ratio and the complex **5** is non-ionic[65].

For complexes **3** and **4**, the ratio for ABT:dipic:M(II) ion:water molecules were obtained from elemental and thermal analyses studies and the structures of these complexes were proposed from UV, magnetic susceptibility and molar conductivity studies (Figure 1). All experimental results are also in good agreement with the X-ray diffraction studies for complexes **2** and **5** (Figures 2 and 3).

In vitro inhibition studies

Inhibitory effects of starting compounds (ABT, H_2dipic) and their complexes (FeABT, CoABT, NiABT, CuABT, Fedipic, Codipic, Nidipic, Cudipic), proton transfer salt (**1**), and its complexes (**2**–**5**) together with AAZ as the control compound were tested on the hydratase and esterase activities of hCA I and hCA II *in vitro*. IC_{50} values were calculated and the results are listed in Table 5.

According to *in vitro* studies, any inhibition effects of all compounds were not observed on hydratase activities of hCA I and hCA II. Also ABT, H_2dipic and metal complexes of H_2dipic did not inhibit the esterase activities of hCA I and hCA II isoenzymes. Against hCA I and hCA II, FeABT, CoABT, NiABT, CuABT and compounds **1**–**5** have shown esterase activities as moderate inhibitors, with IC_{50} values in the range of 0.221–0.746 mM. As shown in Table 5, metal complexes of ABT and novel compounds **1**–**5** are more powerful inhibitors for hCA II than for hCAI. Among the metal complexes of ABT, FeABT is the most effective inhibitor on hCA I and hCA II, with IC_{50} values 0.284 mM and 0.257 mM, respectively. Other metal complexes of ABT have similar inhibitory effects on these isoenzymes (Table 5).

The proton transfer salt (**1**) exhibits inhibition effects on hCA I and II, with IC_{50} values 0.746 and 0.674 mM, respectively. While ABT and H_2dipic do not show any inhibition effects on hCA I and hCA II, the proton transfer salt has considerable inhibition effect due to the structural changes leading to impressive differences of activity[24,26,66]. Similarly, compounds **2**–**5** have more potent effects than all simple metal complexes and compound **1** with nearly three times better inhibition (IC_{50} values 0.241–0.299 mM for hCA I and 0.221–0.281 mM for hCA II) (Table 5)[24,26,66]. The inhibition potentials of **2**–**5** are close to each other; in addition, complex **2** has the most effective inhibition potential among all the newly synthesized compounds (IC_{50} values 0.241 mM for hCA I and 0.221 mM for hCA II).

Conclusions

In this present work, Fe(III), Co(II), Ni(II) as ionic complexes and Cu(II) as mixed ligand complex were prepared for the first time. In complex **2**, the Fe(III) ion coordinates with four oxygen atoms and two nitrogen atoms of two pyridine-2,6-dicarboxylate molecules forming a distorted octahedral conformation. In complex **5**, the Cu(II) ion resides on the center of symmetry in a distorted square-pyramid coordination environment comprising two nitrogen atoms, one from dipic and one from ABT ring, two carboxylate oxygen atoms from dipic and one oxygen atom from water. Intermolecular N–H$\cdots$O and O–H$\cdots$O hydrogen bonds and π–π stacking interactions seem to be effective in the stabilization of the crystal structure. Elemental analyses and all measurements show good agreement with the structures. The structures of **3** and **4** might be proposed as octahedral according to the results of elemental, spectral, magnetic measurement, molar conductivity and thermal analyses.

These five novel compounds possess significant inhibition effect on hCA I and on hCA II for esterase activity, and thus might be considered as possible drugs for glaucoma. These results suggest that further inhibition studies are worthwhile in order to obtain correlation in such compounds and derivatives of such compounds should be subjected to further inhibition *in vivo* tests. The order of inhibition effects increasing through starting compounds and proton transfer salt and the complexes of these compounds might be due to the structural changes leading to impressive difference of activity.

Supplementary data

CCDC 915186 for complex **2** and 915185 for complex **5** contain the supplementary crystallographic data for this article. These data can be obtained free of charge via http://www.ccdc.cam.ac.uk (the Cambridge Crystallographic Data Centre, 12 Union Road, Cambridge CB2 1EZ, UK; Fax: +44 1123 336 033; or Email: deposit@ccdc.cam.ac.uk).

Declaration of interest

The authors report no conflicts of interest. The authors alone are responsible for the content and writing of this article.

The authors acknowledge the support provided by Dumlupınar University Research Fund (grant No. 2010/2). In addition, the authors would like to thank the Medicinal Plants and Medicine Research Center of Anadolu University, for allowing us to use the X-ray facility.

References

1. Prakash A, Adhikari D. Application of Schiff bases and their metal complexes – a review. Int J Chem Tech Research 2011;3:1891–6.
2. He XF, Vogels CM, Decken A, Westcott SA. Pyridyl benzimidazole, benzoxazole, and benzothiazole platinum complexes. Polyhedron 2004;23:155–60.
3. Mortimer CG, Wells G, Crochard JP, et al. Antitumor benzothiazoles.26. 2-(3,4-dimethoxyphenyl)-5-fluorobenzothiazole (GW 610, NSC 721648), a simple fluorinated 2-arylbenzothiazole, shows potent and selective inhibitory activity against lung, colon and breast cancer cell lines. J Med Chem 2006;49:179–85.
4. Premlata VS, Seth G. Synthesis and antibacterial activity of Zn(II) complexes with 2-substituted benzothiazoles and amino acids. J Chem Pharm Res 2012;4:1327–31.
5. Maru M, Shah MK. Synthesis, physico-chemical studies and antimicrobial evaluation of novel 2-(substituted aryl)-1H-benzo[d]thiazoles and their metal(II)chloride complexes. Int J Pharm Pharm Sci 2012;4:388–91.
6. Mathur N, Mathur VK. Species against binuclear *Candida* species against binuclear complexes derived from copper surfactants with azole ring. Int Conf Biol Envir. Chem IPCBEE 2011; 24:133–8.
7. Pal N, Kumar M, Seth G. Biological important Ni(II) ternary complexes derived from 2-substituted benzothiazoles and amino acids. E-J Chem 2011;8:1174–9.
8. Kaur H, Kumar S, Singh I, et al. Synthesis, characterization and biological activity of various substituted benzothiazole derivatives. Digest J Nanomater Biostruct 2010;5:67–76.
9. Paramashivappa R, Phani KP, Rao PVS, Rao S. Replacement of the ureas moiety by benzothiazolesulfonamide provided inhibitors of HIV-1 protease with improved potency and antiviral activities. Bioorg Med Chem Lett 2003;13:657–60.
10. Nagarajan SR, De Crescenzo GA, Getman DP, et al. Discovery of novel benzothiazolesulfonamides as potent inhibitors of HIV-1 protease. Bioorg Med Chem 2003;11:4769–77.
11. Vara-Prasad JVN, Panapoulous A, Rubin JR. Thiocyanation of alkylanilines. A simple and efficient synthesis of thiosulfonates containing 2-aminobenzothiazole. Tetrahedron Lett 2000;41: 4065–8.
12. Maurya RC, Mishra DD. Synthesis and characterization of some novel mixed-ligand cyanonitrosyl $\{CrNO\}_5$ heterocomplexes of chromium(I) with potentially tridentate benzothiazole derivatives. Synth React Inorg Met Org Chem 1992;22:1227–37.
13. Wang N, Lin QY, Feng J, et al. Bis(2-amino-3H-benzothiazolium) bis(7-oxabicyclo[2.2.1]heptane-2,3-dicarboxylato)cobaltate(II) hexahydrate. Acta Cryst 2010;E66:m763–4.
14. Maurya RC, Sharma P, Roy S. Synthesis and characterization of some mixed-ligand picrate complexes of nickel(II) involving

heterocyclic nitrogen donors. Synth React Inorg Metal-Org Chem 2003;33:683–98.
15. Sieron L, Bukowska-Strzyzewska M. Bis(μ-succinato-O,O′:O″,O‴)bis[bis(2-amino-1,3-benzothiazole-N^3)copper(II)]. Acta Cryst 2000;C56:19–21.
16. Sieron L, Bukowska-Strzyzewska M. cis-Bis(2-amino-1,3-benzothiazole-N^3)bis(formato-O,O′)copper(II). Acta Cryst 1999;C55: 167–9.
17. Gu HB, Long L, Li PP, et al. Synthesis, crystal structure and antimicrobial activity of a new ternary copper(II) complex with p-chlorophenoxyacetic acid and 2-amino benzothiazole. Chinese J Struct Chem 2010;29:676–81.
18. Aly AAM, El-Meligy MS, Zidan AS, El-Shabasy M. Thiazoles as complexing agents towards transition metal haloacetates: spectral, magnetic and thermal properties. Anales de Quimica 1990;86: 19–23.
19. El-ajaily MM, El-moshaty FI, El-zweay RS, Maihub AA. New Co(III) mixed ligand complexes effect on the germination and root length of wheat. Int J Chem Tech Research 2009;1:80–7.
20. Büyükkıdan N, Yenikaya C, Sarı M, et al. Synthesis, characterization and biological evaluation of novel Cu(II) complexes with proton transfer salt of 2,6-pyridinedicarboxylic acid and 2-amino-4-methylpyridine. J Coord Chem 2011;64:3353–65.
21. Neelakantan MA, Mariappan SS, Dharmaraja J, Muthukumaran K. pH metric, spectroscopic and thermodynamic study of complexation behavior of 2-aminobenzothiazole with Ni (II) in presence of amino acids. Acta Chim Slov 2010;57:198–205.
22. Shukla SN, Gaur P, Kaur H, et al. Synthesis, spectroscopic characterization and antibacterial sensitivity of some chloro dimethylsulfoxide/tetramethylenesulfoxide ruthenium(II) and ruthenium(III) complexes with 2-aminobenzothiazole. J Coord Chem 2008;1:441–9.
23. Aghabozorg H, Manteghi F, Sheshmani S. A brief review on structural concepts of novel supramolecular proton transfer compounds and their metal complexes. J Iran Chem Soc 2008;5: 184–227.
24. Yenikaya C, Sarı M, İlkimen H, et al. Synthesis, structural and antiglaucoma activity studies of a novel amino salicylato salt and its Cu(II) complex. Polyhedron 2011;30:535–41.
25. Büyükkıdan N, Yenikaya C, İlkimen H, et al. Synthesis, characterization and antimicrobial activity of a novel proton salt and its Cu(II) complex. Russian J Coord Chem 2013;39:24–31.
26. Yenikaya C, Sarı M, Bülbül M, et al. Synthesis, characterization and antiglaucoma activity of a novel proton transfer compound and a mixed-ligand Zn(II) complex. Bioorg Med Chem 2010;18:930–8.
27. Bailey GF, Karp S, Sacks TE. Ultraviolet-absorption spectra of dry bacterial spores. J Bacteriol 1965;89:984–7.
28. Setlow B, Setlow P. Dipicolinic acid greatly enhances production of spore photoproduct in bacterial spores upon UV ırradiation. Appl Environ Microbiol 1993;59:640–3.
29. Waterbury LD, Serrato C, Martinez GR. Effect of bidentate nitrogen heterocycles on dopamine beta-hydroxylase activity *in vitro*. Proc West Pharm Soc 1989;32:9–13.
30. Schuman JS. Antiglaucoma medications: a review of safety and tolerability issues related to their use. Clin Ther 2000;22:167–208.
31. Scozzafava A, Banciu MD, Popescu A, Supuran CT. Carbonic anhydrase inhibitors: inhibition of isozymes I, II and IV by sulfamide and sulfamic acid derivatives. J Enzyme Inhib Med Chem 2000;15:443–53.
32. Supuran CT. Carbonic anhydrases: novel therapeutic applications for inhibitors and activators. Nat Rev Drug Disc 2008;7:168–81.
33. Bülbül M, Saracoğlu N, Küfrevioğlu Öİ, Çiftci M. Bile acid derivatives of 5-amino-1,3,4-thiadiazole-2-sulfonamide as new carbonic anhydrase inhibitors: synthesis and investigation of inhibition effects. Bioorg Med Chem 2002;10:2561–7.
34. Bülbül M, Kasımoğulları R, Küfrevioğlu Öİ. Amide derivatives with pyrazole carboxylic acids of 5-amino-1,3,4-thiadiazole 2-sulfonamide as new carbonic anhydrase inhibitors: synthesis and investigation of inhibitory effects. J Enzyme Inhib Med Chem 2008; 23:895–900.
35. Nuti E, Orlandini E, Nencetti S, et al. Carbonic anhydrase and matrix metalloproteinase inhibitors. Inhibition of human tumor-associated isozymes IX and cytosolic isozyme I and II with sulfonylated hydroxamates. Bioorg Med Chem 2007;15:2298–311.
36. Supuran CT, Scozzafava A. Carbonic anhydrases as targets for medicinal chemistry. Bioorg Med Chem 2007;15:4336–50.
37. Carta F, Vullo D, Maresca A, et al. Mono-/dihydroxybenzoic acid esters and phenol pyridinium derivatives as inhibitors of the mammalian carbonic anhydrase isoforms I, II, VII, IX, XII and XIV. Bioorg Med Chem 2013;21:1564–9.
38. Carta F, Vullo D, Maresca A, et al. New chemotypes acting as isozyme-selective carbonic anhydrase inhibitors with low affinity for the offtarget cytosolic isoform II. Bioorg Med Chem Lett 2012;22: 2182–5.
39. Carta F, Maresca A, Scozzafava A, Supuran CT. 5- and 6-Membered (thio)lactones are prodrug type carbonic anhydrase inhibitors. Bioorg Med Chem Lett 2012;21:267–70.
40. Carta F, Temperini C, Innocenti A, et al. Polyamines inhibit carbonic anhydrases by anchoring to the zinc-coordinated water molecule. J Med Chem 2010;53:5511–22.
41. Kadirova SA, Parpiev NA, Tashkhodzhaev B. Synthesis and spectroscopic and X-ray diffraction studies of complexes of Co(II), Ni(II), Cu(II), and Zn(II) chlorides with benzothiazole derivatives. O'zbekiston Kimyo Jurnali 2008;1:3–9.
42. Campbell MJM, Grzeskowiak R, Juneja, GS. Some iron(III) complexes of 2-aminobenzothiazole. J Inorg Nuclear Chem 1978; 40:1247–9.
43. Anderegg G, Bottari E. Pyridine derivatives as ligands. VII. Complexing tendency of substituted dipicolinate ions. Helvet Chim Acta 1965;48:887–92.
44. Bruker. SADABS. Madison (WI): Bruker AXS Inc; 2005.
45. Sheldrick GM. SHELXS97 and SHEXL97. Program for crystal structure solution and refinement. Germany: University of Göttingen; 1997.
46. Farrugia LJ. ORTEP-3 for Windows – a version of ORTEP-III with a Graphical User Interface (GUI). J Appl Cryst 1997;30:565.
47. Arslan O, Nalbantoğlu B, Demir N, et al. A new method for the purification of carbonic anhydrase isozymes by affinity chromatography. Trop J Med Sci 1996;26:163–6.
48. Rickli EE, Ghazanfar SA, Gibbson BH, Edsall JT. Carbonic anhydrases from human erythrocytes: preparation and properties of two enzymes. J Biol Chem 1964;239:1065–8.
49. Bradford MM. A rapid and sensitive method for the quantitation of microgram quantities of protein utilizing the principle of protein-dye binding. Anal Biochem 1976;72:248–54.
50. Laemmli UK. Cleavage of structural proteins during the assembly of the head of bacteriophage T4. Nature 1970;227:680–5.
51. Wilbur KM, Anderson NG. Electrometric and colorimetric determination of carbonic anhydrase. J Biol Chem 1948;176:147–54.
52. Verpoorte JA, Mehta S, Edsall JT. Esterase activities of human carbonic anhydrases B and C. J Biol Chem 1967;242:4221–9.
53. Innocenti A, Scozzafava A, Parkkila S, et al. Investigations of the esterase, phosphatase, and sulfatase activities of the cytosolic mammalian carbonic anhydrase isoforms I, II, and XIII with 4-nitrophenyl esters as substrates. Bioorg Med Chem Lett 2008;18: 2267–71.
54. Tabatabaee M, Abbasi F, Kukovec BM, Nasirizadeh N. Preparation and structural, spectroscopic, thermal, and electrochemical characterizations of iron(III) compounds containing dipicolinate and 2-aminopyrimidine or acridine. J Coord Chem 2011;64:1718–28.
55. Eshtiagh-Hosseini H, Mirzaei M, Yousefi Z, et al. Structural aspects and solution behavior of metallosupramolecular compound of Fe(III) ion obtained by proton transfer. J Coord Chem 2011;64: 3969–79.
56. Addison AW, Rao TN. Synthesis, structure, and spectroscopic prorerties of copper(II) compounds containing nitrogen–sulphur donor ligands; the crystal and molecular structure of aqua[1,7-bis(N-methylbenzimidazol-2′-yl)-2,6-dithiaheptane] copper(II) perchlorate. Chem Soc J Dalton Trans 1984;1:1349–55.
57. Tamer O, Sariboga B, Ucar I. A combined crystallographic, spectroscopic, antimicrobial, and computational study of novel dipicolinate copper(II) complex with 2-(2-hydroxyethyl)pyridine. Struct Chem 2012;23:659–70.
58. Yenikaya C, Poyraz M, Sarı M, et al. Synthesis, characterization and biological evaluation of a novel Cu(II) complex with the mixed ligands 2,6-pyridinedicarboxylicacid and 2-aminopyridine. Polyhedron 2009;28:3526–32.
59. Yenikaya C, Büyükkidan N, Sari M, et al. Synthesis, characterization, and biological evaluation of Cu(II) complexes with the proton transfer salt of 2,6-pyridinedicarboxylic acid and 2-amino-4-methylpyridine. J Coord Chem 2011;64:3353–65.

60. Cook D. Vibrational spectra of pyridinium salts. Can J Chem 1961; 39:2009–24.
61. Nakamoto K. Infrared and Raman spectra of ınorganic and coordination compounds. 5th ed. NewYork: Wiley-Interscience; 1997.
62. Ucar I, Karabulut B, Bulut A, Buyukgungor O. Synthesis, structure, spectroscopic and electrochemical properties of (2-amino-4-methylpyrimidine)-(pyridine-2,6-dicarboxylato)copper(II) monohydrate. J Mol Struct 2007;834–836:334–6.
63. Swu T. Synthesis through proton transfer reaction, structure and spectroscopic characterization of novel anionic nickel(II) complex with pyridine-2,6-dicarboxylic acid and 4-aminobenzenesulfonamide. J Applicable Chem 2012;1:360–7.
64. Derikvand Z, Dorosti N, Hassanzadeh F, et al. Three new supramolecular compounds of copper (II), cobalt (II) and zirconium (IV) with pyridine-2,6-dicarboxylate and 3,4-diaminopyridine: solid and solution states studies. Polyhedron 2012;43: 140–52.
65. Geary WJ. The use of conductivity measurements in organic solvents for the characterisation of coordination compounds. Coord Chem Rev 1971;7:81–121.
66. Yenikaya C, Sarı M, Bülbül M, et al. Synthesis and characterization of two novel proton transfer compounds and their inhibition studies on carbonic anhydrase isoenzymes. J Inhib Enzyme Med Chem 2011;26:104–11.